A Diode Laser and Modeling Study of Mixed ($CH_4-H_2-O_2$) AC Plasmas

W. Y. Fan,[†] P. F. Knewstubb, M. Käning,[‡] L. Mechold,[‡] J. Röpcke,[‡] and P. B. Davies*

Department of Chemistry, University of Cambridge, Lensfield Road, Cambridge CB2 1EW, U.K.

Received: December 1, 1998; In Final Form: March 16, 1999

Infrared diode laser spectroscopy has been used as a diagnostic probe to measure the concentrations of the methyl radical and stable products in an ac methane/hydrogen/oxygen ($CH_4-H_2-O_2$) plasma. Among the products detected were all of the stable C-2 hydrocarbons and oxygen-containing species including methanol, formaldehyde, formic acid, carbon monoxide, and carbon dioxide. A simple one-dimensional chemical modeling program has been written to calculate and compare the model concentrations of all the detected species with their observed concentrations. Good agreement between these values has been obtained which enables some insights to be gained into the gas-phase mechanism in mixed methane plasmas.

1. Introduction

Hard carbon and graphitic films have been grown extensively in methane chemical vapor deposition (CVD) plasmas.[1,2] Under selected conditions, such as gas mixtures containing up to 5% methane in hydrogen and high substrate temperatures, diamond films have been obtained. Various surface diagnostic techniques such as X-ray diffraction, scanning electron microscopy, and Raman spectroscopy have been used to characterize these carbon films. The mechanism by which the films form from the gas phase has been widely discussed, and transient species, particularly the methyl radical, have been proposed as the essential intermediates. However, the exact mechanism is unknown and, in contrast to the well characterized films themselves, much remains to be done to understand the gas-phase processes. The composition of carbon films can be modified by changing the quantities of hydrogen and oxygen in the plasma. The role of oxygen may be to preferentially etch the graphitic phases by O and OH formed in oxygen-containing plasmas. Recently we showed that the concentration of methyl radicals increases when small amounts of O_2 are added to a CH_4/H_2 ac plasma in a parallel plate deposition reactor.[3] One of the objectives of the present study was to determine the effect of oxygen on other constituents of the plasma and to determine what new oxygen-containing species were generated.

Although the methyl radical is acknowledged to be an important species in carbon CVD, only a few methods are available for its detection in situ. Small transient species such as H, CH, and C_2 have been detected in methane plasmas using optical emission spectroscopy (OES).[4,5] In oxygen-containing hydrocarbon plasmas the well-known OES of OH and CO have been detected, but their ground state concentrations cannot be obtained from OES directly. Polyatomic molecules either have dissociative excited electronic states or have no allowed radiative transitions in the visible region, making OES unsuitable for their detection. Infrared tunable diode laser absorption spectroscopy (TDLAS) is the technique most widely used to detect methyl radicals in their ground state in plasmas. The most convenient band to detect is the well-studied and intense out-of-plane bending mode (ν_2) which has a band origin at 606 cm^{-1}.[6,7]

In pure methane or methane/hydrogen plasmas the main stable product species are the C-2 hydrocarbons, acetylene, ethylene, and ethane.[8] They have been detected by mass spectrometry in particular, and extensive measurements have been reported in pure methane and methane/hydrogen plasmas. How their concentrations are modified in oxygen-containing plasmas has not been well studied, however, and the use of mass spectrometry to deduce the concentrations of, e.g., formaldehyde and methanol, is precluded because their signatures overlap with those of the C-2 hydrocarbons. Most of the molecules expected to exist in $CH_4-H_2-O_2$ plasmas should have infrared active absorption bands so TDLAS becomes the method of choice for these species as well as for methyl. In low pressure plasmas the rotational components of a characteristic molecular vibrational band of low molecular weight polyatomic species can easily be resolved by diode laser spectroscopy. This specificity is essential for analyzing the composition of hydrocarbon plasmas containing oxygen and hydrogen. The TDLAS technique is also very sensitive and can measure concentrations in the plasma as low as 10^{10} cm^{-3} under optimum conditions. This characteristic is also essential in order to detect transient molecules such as the methyl radical and other product molecules which, although stable, may be present only in low concentrations.

In this work diode laser spectroscopy has been used to measure quantitatively the concentrations of the species in $CH_4-H_2-O_2$ plasmas, in which graphitic carbon films are grown, extending earlier work on pure methane ac plasmas in a parallel plate reactor. In addition to the methyl radical and other small hydrocarbon species a number of other constituents of the plasma such as formaldehyde, methanol, and formic acid have been detected. To gain a better understanding of the plasma composition a chemical modeling package has been used to predict the composition of the plasma for comparison with the TDLAS measurements. The results of this study also provide an interesting comparison with a parallel investigation of the same chemical plasma in an electrodeless microwave reactor also using TDLAS.[9]

[†] Present address: Department of Chemistry, University of California, Berkeley, California 94720.

[‡] Permanent address: Institut für Niedertemperatur-Plasmaphysik, Friedrich-Ludwig-Jahn Strasse 19, 17489 Greifswald, Germany.

10.1021/jp984570l CCC: $18.00
Published on Web 05/05/1999

TABLE 1: Vibrational Bands Used to Detect Species in $CH_4-H_2-O_2$ Plasmas. Band Assignments Taken from Ref 11

molecule	vibrational band (cm^{-1})	
CH_3	ν_2	606−608
C_2H_2	ν_5	760−790
C_2H_4	ν_7	945−960
C_2H_6	ν_9	800−820
CO_2	ν_2	600−620
CH_2O	ν_2	1720−1750
HCOOH	ν_3	1720−1750
CO	ν_0	2050−2150
CH_3OH	ν_4	1020−1045

2. Experimental Results

2.1 Plasma Spectroscopy. A diagram and description of the ac parallel plate reactor can be found in ref 10, and only a brief account of it is given here. The precursor gases (CH_4, H_2, O_2) were introduced, either alone or mixed, through a matrix of small holes at the center of the powered (upper) electrode. Typical flow rates and total pressures were 50 to 500 sccm and 0.4 to 1.2 Torr, respectively. The plasma was initiated and sustained using a signal generator at 10 kHz, power amplifier and step-up transformer. Ballast resistors were used to stabilize the discharge, which was operated at currents of up to 100 mA rms, measured in the secondary circuit of the transformer. The diode laser beam was always positioned 1.5 ($\pm$ 0.2) cm above the ground (lower) electrode except for the methyl radical spatial distribution measurements. Three passes of the laser beam across the reactor gave an effective path length of 90 cm in the plasma itself. Absorption spectra were recorded using either mechanical chopping of the diode laser beam or modulation of the diode laser source current. The signal was then demodulated either at the chopper frequency or at twice the diode current modulation frequency (referred to later as 2*f*). The fundamental vibrational bands used for concentration measurements are given in Table 1.[11]

The method of determining the methyl radical concentration has been described earlier.[3,10] Essentially the amplitudes of the methyl radical lines of known line strength were measured against those of N_2O lines also of known line strength and from a measured pressure of the gas. The line strengths of the methyl radical lines were referenced to the measured value of the Q (8,8) line at 300 K. The concentrations of the stable molecules in the plasma were measured by introducing a known pressure of the molecule into the plasma chamber at room temperature (with excitation off) and comparing the signal intensity with the spectrum recorded in the plasma. Measurements of line widths in the plasma and at room temperature were essentially the same (see later). This implies that the translational and rotational temperatures of the plasma species were similar to room temperature, so the line strengths of the transitions used for plasma diagnostics were assumed to be the same as at room temperature. The stable molecules can diffuse out of the plasma where they are formed to occupy completely the space between the mirrors, in which case the effective path length is 150 cm, i.e., the same as when the cell was filled with the pure stable gas. Measurements were always made at pressures sufficiently low to ensure that the 2*f* signal was proportional to the gas concentration. Intense absorption lines (>20% absorption) were not used for concentration measurements to avoid saturation effects. Although stable molecules could readily be detected in the plasma using chopper modulation, second derivative detection was the preferred method because it gave bigger signal-to-noise ratios and was therefore better able to define small changes in the concentrations under different plasma conditions.

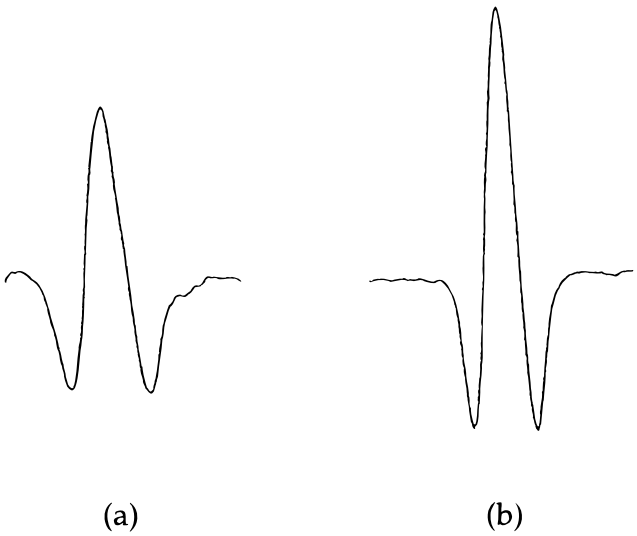

Figure 1. Diode laser lines of (a) methanol ($\sim$ 1033 cm^{-1}) and (b) ethylene ($\sim$ 950 cm^{-1}) recorded using 2*f* modulation in a methane (400 mTorr), hydrogen (300 mTorr), and oxygen (300 mTorr) plasma.

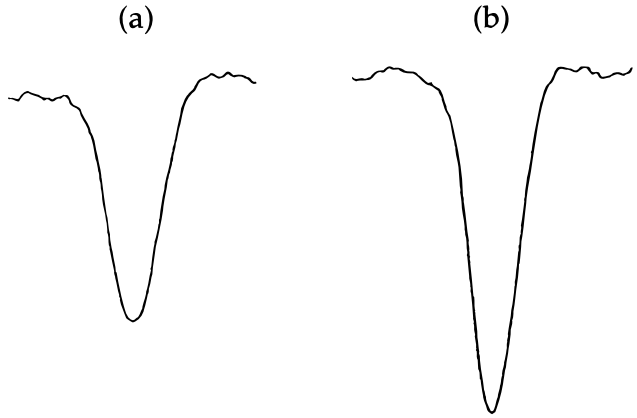

Figure 2. Acetylene absorption line recorded with chopper modulation (a) in a 500 mTorr methane plasma and (b) in a reference gas cell at room temperature and at 20 mTorr. The full width half-maximum of the lines is 0.0025 $\pm$ 0.0003 cm^{-1}.

Usually several ro-vibrational lines were used to monitor and calibrate each species. Figure 1 shows representative 2*f* absorption signals of methanol and ethylene in $CH_4-H_2-O_2$ plasmas.

A knowledge of the translational temperature of the plasma species is useful because many of the reactions involved have strong temperature dependencies. This was done by measuring the widths of selected lines at pressures below $\sim$ 2 Torr where the dominant contribution to the line width is the Doppler effect. For example, the calculated full width half-maximum for an acetylene line is 1.8×10^{-3} cm^{-1}. An instrumental contribution to the line width was also identified and corrected for. Figure 2 shows a line of acetylene in a methane plasma, recorded using chopper modulation and when 20 mTorr of acetylene was placed in the reactor at room temperature. The acetylene line has virtually the same width in both cases, implying that the plasma is close to room temperature. Because the contribution of the instrumental broadening is sometimes difficult to quantify accurately the temperature derived from the line width has quite a large uncertainty of 50 K. The acetylene line width remained virtually unchanged even at higher currents. The translational or gas temperature adopted here is therefore 325 $\pm$ 25 K. For comparison Haverlag et al.[12] have estimated the gas temperature in a CF_4 ac plasma to be within 50 K of room temperature.

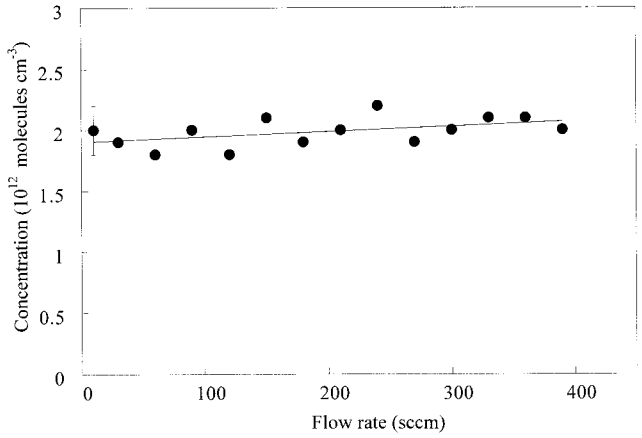

Figure 3. Variation of the methyl radical concentration with flow rate in a pure methane plasma at constant pressure (0.5 Torr) and current (70 mA).

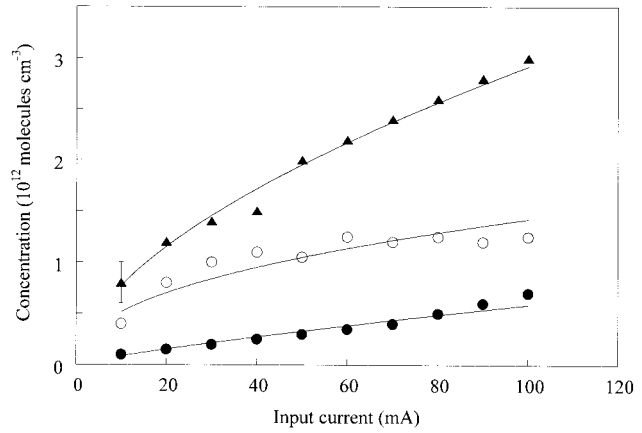

Figure 4. Variation of the methyl radical concentration with applied current in pure methane plasmas at a constant flow rate of 30 sccm of methane. Methane pressures: ▲, 0.19 Torr; ○, 0.51 Torr; ●, 1.03 Torr.

2.2 Methyl Radical Concentration Measurements without Oxygen. *Effects of Flow and Current.* Figure 3 shows the variation of the methyl concentration with flow rate at constant methane pressure. Only very small changes in the methyl concentration occurred, indicating that any loss due to flow out of the reactor was insignificant. Holbrook et al.[13] have reviewed the methyl recombination reaction data at different temperatures and pressures, and their data provides a value for the recombination rate constant under our plasma conditions of temperature and pressure. Comparing this with the reciprocal of the residence time of CH_3 in the reactor (0.1 to 2 s), it is easy to show that the self-recombination reaction occurs much more rapidly than the transport of CH_3 out of the reaction zone. Yamada and Hirota[14] also showed that chemical recombination was the main removal step for methyl in a pulsed discharge where the methyl concentration followed a second-order decay when the discharge was extinguished.

In earlier work[10] the effect of increasing current on the concentration of the methyl radical was investigated at a fixed pressure of 220 mTorr and increasing flow rates in a pure methane plasma. The $[CH_3]$ in a pure methane plasma increased with increasing current at three different pressures and a fixed flow rate, Figure 4. In general $[CH_3]$ increased linearly or almost linearly with current, and there was no sign of saturation of the concentration up to the highest currents used (100 mA). The observation that the lowest pressure data in Figure 4 gave the highest methyl radical concentrations can be attributed to the smaller methyl recombination rate at lower pressures and higher electron energies, leading to more effective methane dissociation. The current dependence in Figure 4 is in accord with the increasing density of electrons. A similar conclusion was reached by Kline et al.[15] who observed a linear increase in [e] with increasing current in a methane rf plasma.

The major reactions that control the methyl radical concentration in a pure methane plasma are

$$CH_4 + e = CH_3 + H + e \qquad k_{1e}$$

and

$$CH_3 + CH_3 + M = C_2H_6 + M \qquad k_2$$

where M is the concentration of methane. It can readily be shown that the ion−molecule reaction $CH_4^+ + CH_4 = CH_3 + CH_5^+$ makes only a small contribution to the rate of formation of CH_3 because the ionization energy of methane to form CH_4^+ is almost 3 eV higher than the electron impact dissociation energy to form $CH_3 + H$. Even though the recombination reaction $CH_5^+ + e = CH_3 + H_2$ is rapid ($k = 3 \times 10^{-7}$ cm^3 s^{-1})[16] it would require an unreasonably large $[CH_5^+]$, namely 1×10^{13} cm^{-3}, for this reaction to be a significant source of methyl radicals compared with electron impact (k_{1e}). This is a low-temperature, low-pressure plasma with typical degrees of ionization between 10^{-4} and 10^{-6}, i.e., with the total concentration of ions of order 10^{10} cm^{-3}. Assuming that the simple model above is valid for controlling $[CH_3]$, then if the methyl radical concentration is put in the steady state,

$$[CH_3] = (k_{1e}[e][CH_4]/2k_2[M])^{1/2} \qquad (1)$$

This equation combined with data such as that in Figure 4 can be used to calculate $k_{1e}[e]$. For example, at a fixed current of 100 mA values of $k_{1e}[e]$ are 6.2×10^{-2}, 1.2×10^{-2}, and 3.5×10^{-3} s^{-1} at pressures of 190, 510, and 1030 mTorr, respectively. The values for $k_2[M]$ were taken from ref 13 at the appropriate pressure and temperature. It is emphasized that these are only approximate values of $k_{1e}[e]$ because of the assumptions involved. The addition of oxygen and the state of the electrode surfaces were observed to affect the measurements of $[CH_3]$, for example. Nevertheless, bearing in mind the large uncertainty in the line strength of the CH_3 transitions used (30%), the $k_{1e}[e]$ values are adequate approximations for the present purposes.

Spatial Measurements. The only spatial concentration measurements made in the reactor were of the methyl radical in pure methane plasmas at different pressures. The concentration was measured in incremental steps of 5 mm from the powered electrode to the ground electrode. Figure 5 shows the results using the Q (3,3) line of methyl. At all pressures the concentration was found to be independent of flow rate, i.e., the same for 30 sccm as for 300 sccm of methane. This confirmed that transport effects are unimportant in removing the methyl radical. The methyl radical concentration was uniform across the plasma at low pressures, while at higher pressure a minimum was observed in the center of the reactor for observations along the electric field direction. We have no data on the radial variation. The concentration of the methyl radical reflects the profile of the electron energy distribution across the plasma. Higher energy electrons, and therefore methyl radicals, are more abundant in the negative glow region. At low pressure the negative glow, which in the methane plasma is a purple-colored emission, uniformly fills the space between the two electrodes. Under these conditions the methyl concentration was essentially constant

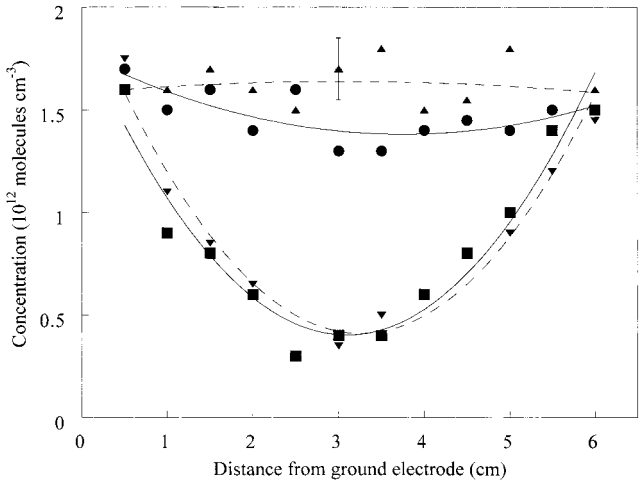

Figure 5. Variation of the methyl radical concentration at various distances above the ground electrode measured as a function of pressure and flow rate. ■, 700 mTorr, 30 sccm; ▼, 700 mTorr, 300 sccm; ●, 200 mTorr, 30 sccm; ▲, 200 mTorr, 300 sccm. A representative uncertainty in the concentrations is indicated.

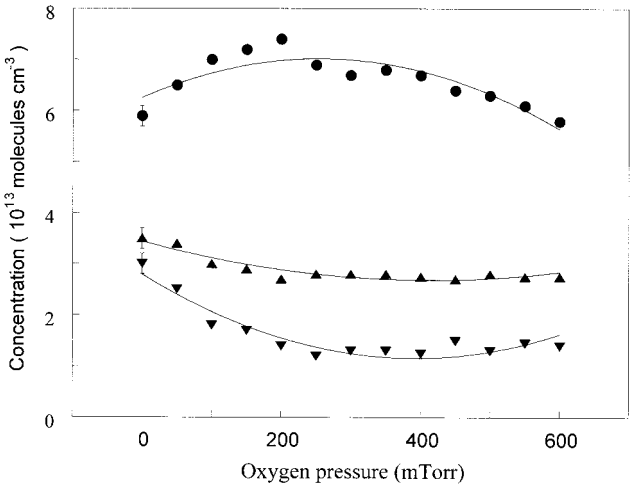

Figure 6. The concentrations of ethane (●), ethylene (▲), and acetylene (▼) in a $CH_4-H_2-O_2$ plasma. Representative error bars are shown. The pressure of methane was fixed at 400 mTorr and the P_{H_2}/P_{O_2} ratio was varied to keep the total pressure in the reactor constant at 1 Torr.

across the plasma. At higher pressures the electrons lose more energy because of collisions, and the negative glow is restricted to the space near both electrodes. Electrons in the Faraday dark space in the middle of the reactor have lower energies and generate fewer methyl radicals by electron impact.

The methyl concentration across the reactor at the higher pressures can be predicted using a simple model for the behavior of the radical. Assuming that the methyl radical is formed by electron impact and removed by recombination and diffusion we have:

$$\frac{d[CH_3]}{dt} = k_{1_e}[e]\,[CH_4] - 2k_2\,[CH_3]^2[M] - D\frac{d^2[CH_3]}{dx^2} \quad (2)$$

where D is the diffusion coefficient of methyl in methane and x the distance from the ground electrode. For the high-pressure case (Figure 5) the concentration was fitted by a parabola of the form $[CH_3] = 1.86 \times 10^{11}(x-3)^2 + 3.65 \times 10^{11}$ molecules cm^{-3} which yields $d^2[CH_3]/dx^2 = 3.72 \times 10^{11}$ molecules cm^{-3}/cm^2. Assuming that the steady state can be applied to $[CH_3]$ in eq 2 then $[CH_3] = \{(k_{1e}[e]\,[CH_4] - 3.72 \times 10^{11}\,D)/2k_2[M]\}^{1/2}$.

The diffusion coefficient of methyl in methane at 1 Torr is ~ 115 cm^2 s^{-1}, $[CH_3] \sim 1.6 \times 10^{12}$ molecules cm^{-3} at $x = 1$ (Figure 5), and $k_2\,[M] \sim 5 \times 10^{-11}$ cm^3 $molecule^{-1}$ s^{-1} so that $k_{1e}[e] = 0.12$ s^{-1}. This value hardly changes if $D = 0$, showing that diffusion of the methyl radical is an unimportant loss process. Although the diffusion coefficient will be larger at lower total pressures, this effect will be counter-balanced by smaller methyl concentration gradients.

Gogolides et al.[17] have developed a combined physical and chemical predictive model of a methane rf plasma applicable at pressures up to 300 mTorr. It was applied to CH_3 and CH_2 (and CH_4 and H) in a parallel plate reactor, and the results compared with the experimental spatial profiles reported by Sugai and Toyoda.[18] At the highest pressures (300 mTorr) the profiles are predicted to peak very close to the electrodes with a pronounced dip midway between the electrodes. At the lowest pressures (57 mTorr) the dip in concentration had disappeared for methyl and was less pronounced for methylene. The absolute experimental concentrations were in satisfactory agreement with the modeling for CH_2 but less satisfactory for CH_3. The results reported here in Figure 5 at 700 mTorr and 200 mTorr are comparable with the modeled profiles at 300 and 57 mTorr respectively.[17] The absolute concentrations of methyl are in fact very close to the modeled values, i.e., between 1 and 2×10^{12} cm^{-3}. On the other hand the CH_2 concentrations were modeled at 100 times less which could explain why they were not observed either in the ac or rf reactors.

2.3 Molecule Concentrations in $CH_4-H_2-O_2$ Plasmas. *Methyl Radical.* The change in the methyl radical concentration as a function of the oxygen partial pressure in a $CH_4-H_2-O_2$ plasma was investigated at a fixed total pressure of 1.0 Torr. The detailed results have been reported earlier.[3] In brief, three sets of measurements were performed at three different pressures of methane. Relatively small flows of oxygen were added, and the hydrogen flow rate was reduced to maintain a constant total pressure. The most important observation was a sharp increase in the methyl concentration (by as much as 75%) at very low additions of O_2. The methyl radical concentration then gradually decreased with further additions of oxygen. In contrast, in an electrodeless $CH_4-O_2-H_2$ microwave plasma no initial maximum was observed, and the methyl radical concentration decreased monotonically as the oxygen flow rate increased.[9] This observation was explained earlier by an increase in the cathode fall potential rather than by chemical/mechanistic factors, and this proposition seems to be borne out by the absence of a similar increase in the electrodeless microwave reactor.

C-2 Hydrocarbons: C_2H_2, C_2H_4, C_2H_6. The C-2 hydrocarbon concentrations were measured as a function of increasing amounts of oxygen (Figure 6). These measurements were carried out at a fixed partial pressure of 400 mTorr of methane while the H_2 and O_2 flow rates were adjusted to keep the total pressure constant at 1 Torr. A fixed current of 100 mA was used. The concentration of ethane increased gradually to a maximum at around 100 mTorr O_2. In previous work[3] we showed that the addition of small amounts of oxygen rapidly increased the concentration of the methyl radical in $CH_4-H_2-O_2$ plasmas. The main reaction removing methyl, at least in the absence of oxygen, is self-recombination to produce ethane. The increase in ethane as a function of added oxygen was generally less than 20% of $[C_2H_6]_{O_2=0}$, and its increase was certainly much less pronounced than for methyl. The C_2H_2 and C_2H_4 concentrations just decreased to a near constant value as P_{O_2} was increased. When the concentration of methane was doubled the same

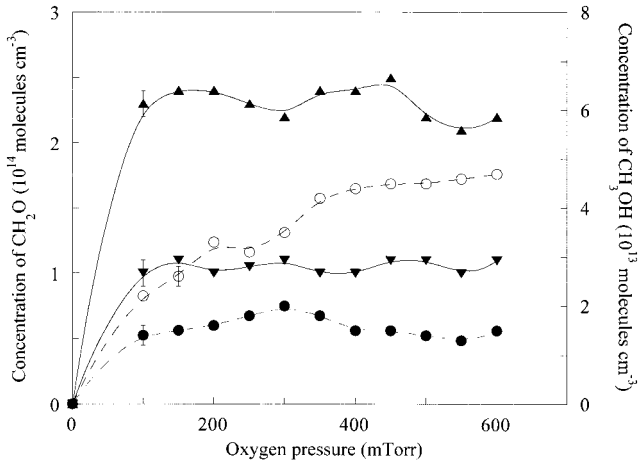

Figure 7. The concentrations of formaldehyde and methanol in a $CH_4-H_2-O_2$ plasma as the pressure of oxygen was varied. Formaldehyde data at methane pressures of ▼, 200 mTorr and ▲, 400 mTorr. Methanol data at methane pressures of ●, 200 mTorr and ○, 400 mTorr. The ratio P_{H_2}/P_{O_2} was varied to keep the total pressure constant at 1 Torr. (Data points have been connected only as a guide to the eye.)

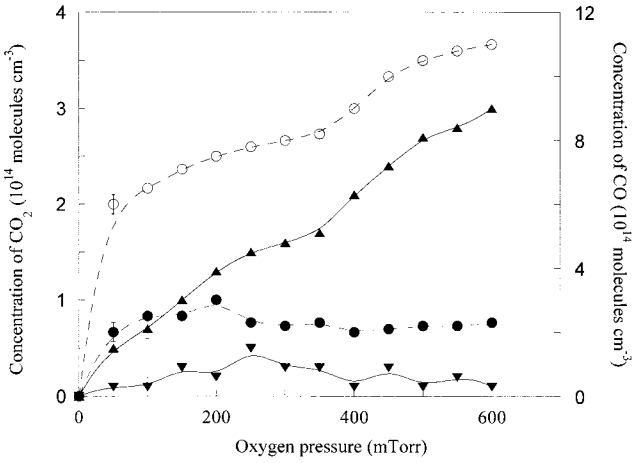

Figure 8. The concentrations of CO and CO_2 in a $CH_4-H_2-O_2$ plasma as the pressure of oxygen was varied. CO data at methane pressures of ●, 200 mTorr and ○, 400 mTorr. CO_2 data at methane pressures of ▼, 200 mTorr and ▲, 400 mTorr. The ratio P_{H_2}/P_{O_2} was varied to keep the total pressure constant at 1 Torr. (Data points have been connected only as a guide to the eye.)

general trends were observed for increasing oxygen concentrations as seen in Figure 6.

Carbon deposits were produced in copious amounts in the plasma chamber even after short discharge periods. To check whether these deposits could have been a source of C-2 species when the plasma was active it was operated with just hydrogen and oxygen. No absorptions due to C-2 species were detected, confirming that the hydrocarbons originated from the gas phase plasma chemistry. When the reactor had been thoroughly cleaned and measurements repeated, the concentrations and their variations were identical to the results from the coated reactor to within experimental accuracy. The results for the C-2 product hydrocarbons illustrate the differences between the electrodeless microwave plasma and the present experiments under similar, but not exactly identical, conditions of flow, pressure, etc. In microwave plasmas containing methane, hydrogen, and argon the highest concentration C-2 species was ethane followed by acetylene and ethylene.

Oxygen-Containing Products. Using TDLAS five other stable molecules were detected in the plasma in the presence of oxygen. They were formaldehyde, formic acid, methanol, carbon monoxide, and carbon dioxide. The concentrations of these species were measured under the same operating conditions as the C-2 hydrocarbon measurements (Figure 6). The presence of formaldehyde is not surprising because one of its source reactions is the reaction of oxygen atoms with the methyl radical. The final products of reaction are CO and CO_2 which give an indication of how much methane has been completely oxidized. The detection of formic acid was not expected because this species is not a prominent product of hydrocarbon combustion. Little is known about its chemistry in plasmas.

Figure 7 shows the concentration of formaldehyde at different oxygen flow rates and for two fixed methane pressures. The concentration of formaldehyde is essentially constant at a particular methane pressure. The concentration data points in Figure 7 show considerable scatter due to instability in the diode laser used. The measurements were repeated many times with the same random fluctuations. The concentrations of methanol formed are lower than formaldehyde under the same conditions. At the higher flow rate of methane the methanol concentration depends slightly on the oxygen flow rate, Figure 7. In the corresponding microwave plasma the formaldehyde concentrations were 100-fold lower and no methanol was observed. The latter may simply have reflected the lower concentration of methanol in the microwave plasma, i.e., below the detection limit. Despite the large differences in formaldehyde concentrations a similar lack of a strong dependence of $[CH_2O]$ on the flow rate of oxygen was noted in both types of plasma.

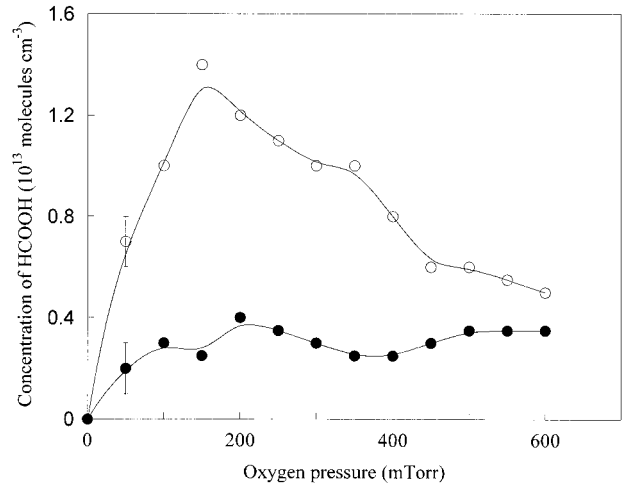

Figure 9. The concentration of formic acid in a $CH_4-H_2-O_2$ plasma at pressures of methane of (●) 200 mTorr and (○) 400 mTorr. The total pressure was maintained at 1 Torr. (Data points have been connected only as a guide to the eye.)

Figure 8 shows the concentrations of CO and CO_2 as oxygen was added. Only at the higher pressure of methane was there a dependence on the flow rate of oxygen. The amount of CO was always higher than CO_2. Formic acid has the lowest concentration of any of the stable molecules, Figure 9. Its concentration variation with the oxygen flow rate shows a maximum at the higher methane flow, at an approximate methane/oxygen ratio of 4:1. In contrast, formic acid was not detected in the methane microwave plasma under similar conditions. The absorption signals of CH_3OH, CH_2O, CO, CO_2, and HCOOH all disappeared when the oxygen or methane flow was stopped with the plasma active.

3. Plasma Modeling

3.1 Outline of the Model. The 1-D FACSIMILE program used earlier has been extended to $CH_4-H_2-O_2$ plasmas with

TABLE 2: Calculated Effective Diffusion Coefficients at 1 Torr Total Pressure and 325 K in Pure Methane or Hydrogen or Oxygen. Values Are Rounded to the Nearest 5 cm^2 s^{-1}

	diffusion coefficient (cm^2 s^{-1})/bath gas		
diffusing molecule	CH_4	H_2	O_2
CH_3	115	225	85
CH_4	110	225	80
C_2H_2	65	125	40
CO	150	375	120
C_2H_4	60	115	40
CH_2O	90	200	65
C_2H_6	55	110	35
CH_3OH	60	120	35
CO_2	85	200	60
HCOOH	55	120	35

the aim of calculating the concentrations of oxygen-containing species as well as product hydrocarbons.[10] The model is based on a plug flow reactor with the space between the powered electrode and the ground electrode divided into seven parallel, 1-cm thick volume elements. Within each volume element the concentration, C, of an individual species is governed by

$$\frac{dC}{dt} = Q + D\left(\frac{d^2C}{dx^2}\right) - u\left(\frac{dC}{dx}\right) \quad (3)$$

where Q is the net rate of formation and removal of the species by chemical reaction, D its diffusion coefficient, and u the flow velocity. To evaluate the partial differential, eq 3 has to be changed into a set of ordinary differential equations based on the method of finite volume. Details can be found in ref 19. Essentially the method involves integrating and averaging over each of the elements into which the reactor volume has been divided. For most measurements the TDLAS technique was used to determine the concentrations in the negative glow region near the ground electrode, corresponding to the first row modeled by FACSIMILE. The radial distribution was assumed to be uniform in the model. It cannot be determined experimentally anyway because TDLAS measures an average species concentration parallel to the electrodes. The distribution of the methyl radical in the electric field direction in a pure methane plasma was also modeled for comparison with experiment (Figure 5).

3.2 Diffusion and Flow. The diffusion coefficients of hydrocarbon species in methane required for eq 3 were calculated using the standard expression[20]

$$D = 0.375\lambda\left(\frac{\pi kT}{2\mu}\right)^{1/2} \quad (4)$$

where λ is the mean free path of the molecule of interest and μ the reduced mass of the molecule and the bath gas. The value of λ for pure methane is 3.9×10^{-3} cm at 1 Torr, corresponding to a collision cross-section (σ) of 7×10^{-15} cm^2.[21] The values of D for oxygen and hydrogen atoms were calculated using the same cross-section, and for larger molecules such as the C-2 hydrocarbons D was calculated by scaling the value for methane by the ratio of the molecular radii. Table 2 gives the calculated diffusion coefficients for methyl and various stable molecules in methane, hydrogen, and oxygen. When mixtures of gases were being used, such as methane, hydrogen, and oxygen, an effective diffusion coefficient, D_{eff}, was calculated using

$$\frac{1}{D_{eff}} = \frac{x}{D_{CH_4}} + \frac{y}{D_{H_2}} + \frac{z}{D_{O_2}} \quad (5)$$

where x, y, and z are the appropriate mole fractions. The calculated values of D_{eff} for each of the molecules in Table 2 in a 4:3:3 mixture of $CH_4/H_2/O_2$ at 1 Torr are given in Table 3.

TABLE 3: Calculated Diffusion Coefficients at 1 Torr Total Pressure and 325 K in a 4:3:3 Mixture of Methane, Hydrogen, and Oxygen. Values Are Rounded to the Nearest 5 cm^2 s^{-1}

molecule	effective diffusion coefficient (cm^2 s^{-1})
CH_3	120
CH_4	115
C_2H_2	60
CO	165
C_2H_4	55
CH_2O	95
C_2H_6	50
CH_3OH	55
CO_2	90
HCOOH	55

The residence time, τ_p, of atoms and molecules determined by mass flow was calculated using

$$\tau_p = VP273/QT$$

where V is the reactor volume, P the gas pressure, and Q the flow rate through the reactor. The flow velocity, u, was calculated by dividing the electrode spacing (7 cm) by the residence time. The residence time of individual species was assumed to be the same as for the bulk flow of gas.

3.3 Contributing Reactions. In the $CH_4-H_2-O_2$ plasma electron impact dissociation of the three parent molecules initiates the plasma chemistry. These and other electron impact processes are described in the next section. Only the neutral reactions are mentioned here. To arrive at a manageable number of these reactions for modeling, they were selected on the basis of the magnitude of their rate coefficients and their known or estimated reactant concentrations. The reaction scheme for the non-oxygen-containing species follows that of Kline, Partlow and Biess[15] for CH_4-H_2 plasmas. The rate coefficients were taken from the comprehensive compilation by Baulch et al.[22] About forty neutral reactions were included in the model (Table 4); some of these reactions do not produce stable product molecules.

The methyl radical itself plays a central role in the plasma chemistry. In the absence of oxygen it is removed by self-recombination and to a lesser extent by reaction with H, but in the presence of oxygen atoms it reacts rapidly to form formaldehyde (reactions 2, 3, and 20 in Table 4). In turn formaldehyde reacts with oxygen and hydrogen atoms and with hydroxyl radicals to yield HCO, CO, and ultimately CO_2. Reactions such as $H + O_2 = OH + O$ may not lead directly to the formation or removal of the detected stable species, but they are important for controlling the concentrations of the transient species in the plasma. Unfortunately the IR active transitions of OH lie at the upper end of the frequency coverage of lead salt diode lasers, and so the concentrations of OH (and of H and O) have to be inferred from the model itself. Another important free radical suggested by the modeling predictions is HCO, but this has not yet been detected. Oxygen and hydrogen atoms are involved in many more gas-phase reactions than the molecular radicals and are also more surface active, hence their concentrations are more difficult to predict. For convenience it was useful to collect the dominant reactions responsible for particular product molecules into groups and these are given in Table 5.

3.4 Electron Impact Dissociation Reactions. In contrast to the extensive rate data on the reactions of atomic oxygen and hydrogen with neutral hydrocarbons and related plasma mol-

TABLE 4: Elementary Reactions Used to Model $CH_4-H_2-O_2$ Plasmas. Rate Constants Have Been Taken from Ref 22 and Calculated for 325 K[a]

reaction no.	reaction	k_{325} cm^3 molecule^{-1} s^{-1}
	hydrocarbon and hydrogen reactions	
1	$CH_4 + H = CH_3 + H_2$	3.0×10^{-18}
2	$CH_3 + CH_3 + (M) = C_2H_6 + (M)$	5.0×10^{-11a}
3	$CH_3 + H + (M) = CH_4 + (M)$	2.1×10^{-12a}
4	$CH_3 + H_2 = CH_4 + H$	4.0×10^{-20}
5	$C_2H_6 + H = C_2H_5 + H_2$	1.5×10^{-16}
6	$C_2H_5 + H_2 = C_2H_6 + H$	9.5×10^{-18}
7	$C_2H_5 + H = C_2H_4 + H_2$	6.0×10^{-11}
8	$C_2H_4 + H = C_2H_3 + H_2$	8.6×10^{-20}
9	$C_2H_3 + H_2 = C_2H_4 + H$	9.6×10^{-17}
10	$C_2H_3 + H = C_2H_2 + H_2$	2.0×10^{-11}
11	$CH + CH_4 = C_2H_4 + H$	9.3×10^{-11}
12	$C_2H + H_2 = C_2H_2 + H$	7.0×10^{-11}
	reactions involving oxygen	
13	$OH + O = O_2 + H$	2.8×10^{-11}
14	$O + H_2 = OH + H$	2.6×10^{-17}
15	$OH + H_2 = H_2O + H$	1.1×10^{-14}
16	$OH + OH = H_2O + O$	1.6×10^{-12}
17	$CH + O_2 = HCO + O$	5.5×10^{-11}
18	$CH_4 + O = CH_3 + OH$	2.5×10^{-17}
19	$CH_4 + OH = CH_3 + H_2O$	1.4×10^{-14}
20	$CH_3 + O = CH_2O + H$	1.4×10^{-10}
21	$CH_2O + H = HCO + H_2$	1.0×10^{-13}
22	$CH_2O + O = HCO + OH$	2.6×10^{-13}
23	$CH_2O + OH = HCO + H_2O$	3.6×10^{-12}
24	$HCO + H = CO + H_2O$	1.5×10^{-10}
25	$HCO + O = CO + OH$	5.0×10^{-11}
26	$HCO + OH = CO + H_2O$	1.7×10^{-10}
27	$HCO + O_2 = CO + HO_2$	5.0×10^{-12}
28	$CO + OH = H + CO_2$	1.3×10^{-13}
29	$C_2H_6 + O = C_2H_5 + OH$	1.2×10^{-15}
30	$C_2H_6 + OH = C_2H_5 + H_2O$	3.3×10^{-13}
31	$C_2H_4 + O =$ products	9.7×10^{-13}
32	$C_2H_4 + OH = C_2H_3 + H_2O$	3.4×10^{-15}
33	$C_2H_2 + O =$ products	1.8×10^{-13}
34	$C_2H_5 + O_2 = C_2H_4 + HO_2$	5.0×10^{-13}
35	$C_2H_3 + O_2 = CH_2O + HCO$	9.0×10^{-12}
36	$CH_3 + OH + M = CH_3OH + M$	1.0×10^{-11a}
37	$CH_3OH + H = CH_3O + H_2$	5.3×10^{-15}
38	$CH_3OH + O = CH_3O + OH$	1.2×10^{-14}
39	$CH_3OH + OH = CH_3O + H_2O$	1.2×10^{-12}

[a] Pseudo second order rate coefficients at 1 Torr, 325 K and with M = Ar.

ecules, there is a dearth of corresponding data for electron impact dissociation reactions of these molecules (Table 6). This arises because of the difficulty of measuring the absolute cross-section of such reactions, and instead the rate coefficients have to be calculated. The only calculated value of k_{1e}, the rate coefficient for the fundamental reaction $CH_4 + e = CH_3 + H + e$, is due to Kline et al. [15] from electron swarm measurements ($k_{1e} = 4.8 \times 10^{-8}$ cm^3 molecule^{-1} s^{-1}). This value was used in the earlier analysis of methane plasmas. The expression for k_{1e} is

$$k_{1e} = \int_0^\infty \left(\frac{2E}{m}\right)^{1/2} (\sigma_{CH_3}(E)) f(E) \mathrm{d}E \qquad (6)$$

where E is the electron energy, $(2E/m)^{1/2}$ its velocity, $\sigma_{CH_3}(E)$ the energy-dependent dissociation cross-section to produce the methyl radical, and $f(E)$ the electron energy distribution. Nakano et al [23] have reported $\sigma_{CH_3}(E)$ based on appearance mass spectra, enabling k_{1e} to be evaluated. The electron energy bi-Maxwellian distribution function reported for CH_4-H_2 plasmas was used as an approximation for $f(E)$.[24] Only the high energy component of this function is required to determine k_{1e} because only the more energetic electrons dissociate methane to methyl. A

TABLE 5: Principal Formation and Removal Reactions for the Species Generated in $CH_4-H_2-O_2$ Plasmas

formation reaction(s)	removal reaction(s)
CH_3 (methyl)	
$CH_4 + e = CH_3 + H + e$	$CH_3 + O = CH_2O + H$
	$CH_3 + CH_3 + M = C_2H_6 + M$
C_2H_6 (ethane)	
$CH_3 + CH_3 + M = C_2H_6 + M$	$C_2H_6 + e = C_2H_5 + H + e$
C_2H_4 (ethylene)	
$CH + CH_4 = C_2H_4 + H$	$C_2H_4 + e = C_2H_3 + H + e$
	$C_2H_4 + e = C_2H_2 + H_2 + e$
C_2H_2 (acetylene)	
$C_2H_4 + e = C_2H_2 + H_2 + e$	$C_2H_2 + e = C_2H + H + e$
CH_2O (formaldehyde)	
$CH_3 + O = CH_2O + H$	$CH_2O + e = HCO + H + e$
	$CH_2O + H = HCO + H_2$
	$CH_2O + O = HCO + OH$
	$CH_2O + OH = HCO + H_2O$
CH_3OH (methanol)	
$CH_3 + OH + M = CH_3OH + M$	$CH_3OH + e = CH_3O + H + e$
CO (carbon monoxide)	
$HCO + O_2 = CO + HO_2$	$CO + OH = H + CO_2$
CO_2 (carbon dioxide)	
$CO + OH = H + CO_2$	$CO_2 + e = CO + O + e$
HCOOH (formic acid)	
$HOCO + H + M = HCOOH + M$	$HCOOH + e = HOCO + H + e$
$O + CH_2O = HCOOH$	

TABLE 6: Calculated Values of the Electron Impact Dissociation Rate k[e] Used in the Chemical Model

reaction no.	reaction	k[e] s^{-1}
1	$CH_4 = CH_3 + H$	0.45
2	$CH_4 = CH_2 + H_2$	0.45
3	$CH_4 = CH + H_2 + H$	0.18
4	$C_2H_6 = C_2H_5 + H$	2.0
5	$C_2H_4 = C_2H_3 + H$	0.4
6	$C_2H_4 = C_2H_2 + H_2$	1.6
7	$C_2H_2 = C_2H + H$	2.0
8	$CH_2O = HCO + H$	2.0
9	$CH_3OH = CH_3O + H$	2.0
10	$HCOOH = HOCO + H$	2.0
11	$CO_2 = CO + O$	0.45

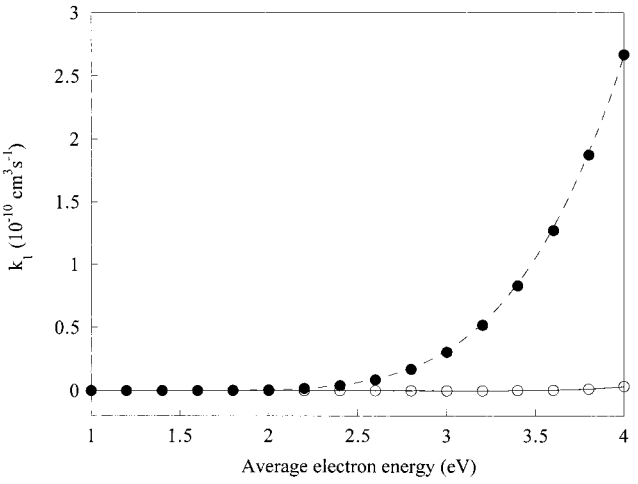

Figure 10. Calculated values of k_1 as a function of average electron energy for the Maxwellian (●) and Druyvestyn (○) distributions.

numerical integration of eq 6 using Simpson's rule was used to calculate k_{1e} as a function of E_{av}, the average electron energy (Figure 10). The cross-section data from Nakano et al.[23] was used unmodified. (The Druyvestyn distribution is also shown

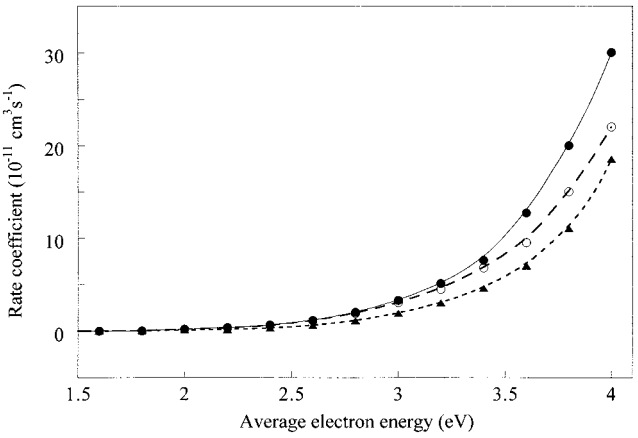

Figure 11. Calculated rate coefficients for the electron impact dissociation of methane to CH_3 (●), CH_2 (○), and CH (▲).

in Figure 10 for completeness.) Specific values of k_{1e} at particular E_{av} are then easily obtained.

Information on E_{av} in methane plasmas is sparse because Langmuir probe measurements are impaired by deposition on the probe. However, E_{av} for argon and helium plasmas is known. A Langmuir probe was used to find the electron density and electron temperatures in a pure argon plasma in our reactor, under similar flow conditions and applied power levels as used for the pure methane and mixed methane ac plasmas. The electron density and average energy were found to be in the range 0.4 to 1.3 $\times$ 10^{10} cm^{-3} and 2.8 to 3.4 eV, respectively. The thermal electron density was assumed to be the same in the methane-containing plasmas, enabling k_{1e} itself to be evaluated. For example, with $I = 50$ mA and a methane pressure of 0.19 Torr, the value of k_{1e}[e] deduced from the kinetics controlling [CH_3] described in section 2.2 is 0.031 s^{-1}, giving $k_{1e} = 3.1 \times 10^{-12}$ cm^3 molecule^{-1} s^{-1} if [e] = 1×10^{10} cm^{-3}. This value of k_{1e} corresponds to average electron energies of 2.3 and 4.0 eV for the Maxwellian and Druyvestan distributions, respectively (Figure 10). The rate coefficient for the dissociation of methane to methylene can be calculated in an analogous fashion using the cross-section of Nakano et al.[23] for the dissociation of methane to methylene. The result shows (Figure 11) that for average energies between 2 and 4 eV the rate coefficient is about 90% of the value for dissociation to methyl.

Calculating the electron impact dissociation to form the CH free radical presents more of a problem because to the authors' knowledge this cross-section has not been measured. The threshold dissociation energies for producing methyl or methylene from methane are very similar (~9.8 eV) as are the bond dissociation energies $\Delta H \sim 4.6$ eV. In contrast the bond dissociation energy to form CH is more endothermic, namely, 7.5 eV. If a linear proportionality is assumed between the enthalpy and the electron impact dissociation energy, then this yields a threshold electron impact dissociation energy for forming CH of 12.8 eV. Assuming the same cross-section profile as for forming methyl, this gives the rate coefficient shown in Figure 11. The qualitative result then is that electron impact dissociation of methane yields CH_3, CH_2, and CH in roughly similar quantities.

Kline et al.[15] calculated the rate coefficients for electron impact dissociation of acetylene, ethylene, and ethane in the electron swarm model to be about four times greater than for the dissociation of methane. Unfortunately they did not report the electron energy dependence of the rate coefficients, but scaling up our value for methane dissociation by the same factor

TABLE 7: Experimental and Modeled Concentrations (molecules cm^{-3}) of the Species Formed in a $CH_4-H_2-O_2$ Plasma

molecule	exptl concn	modeled concn
CH_3	2.2×10^{12}	1.7×10^{12}
C_2H_6	7.0×10^{13}	6.2×10^{13}
C_2H_4	3.1×10^{13}	3.6×10^{13}
C_2H_2	1.4×10^{13}	1.8×10^{13}
CH_2O	2.2×10^{14}	3.1×10^{14}
CH_3OH	3.5×10^{13}	1.4×10^{13}
CO	8.1×10^{14}	9.9×10^{14}
CO_2	1.5×10^{14}	2.1×10^{14}
HCOOH	9.0×10^{12}	7.0×10^{12}

provides qualitative results for the C-2 hydrocarbon dissociation. Dagel et al.[25] found two major channels for the dissociation of ethylene, $C_2H_4 + e = C_2H_2 + H_2 + e$ and $C_2H_4 + e = C_2H_3 + H + e$, but could not determine the branching ratio accurately. As an approximation the branching ratio was again based on the relative endothermicity of the reactions. With this approximation the latter reaction contributes 80% of the total rate coefficient.

With the exception of CO_2 the rate coefficient for electron impact dissociation of other molecules containing H, C, and O were given the same values as the C-2 hydrocarbons. The much higher bond energy in CO_2 suggests a smaller electron impact dissociation rate, and it was fixed at the value for dissociating methane to methyl. The electron impact dissociation energy of CO is sufficiently high that this step has been omitted from the electron impact terms. The cross-sections for hydrogen and oxygen are available in the literature, and their calculated rate constants were similar in magnitude to the dissociation of methane to methyl at low (2−4 eV) electron energies.

3.5 Model Parameters and Results. Both fixed and variable model parameters were used for predictions. The fixed parameters were the rate coefficients at 325 K (Table 4), the diffusion coefficients (Tables 2 and 3), and the flow velocity. There were two groups of variable parameters. First the concentrations of the oxygen and hydrogen atoms. These not only react with almost all of the molecules in the plasma but are also surface active so a heterogeneous rate term was introduced. Their concentrations could be varied by adjusting their surface sticking coefficients. The other group of variables were the k[e] terms for each electron impact reaction. Because the values for the C-2 hydrocarbons and C−H−O-containing molecules were scaled from the electron impact of methane to methyl only the latter was varied. Similarly the dissociation to methylene was set equal to k_1[e] while that for dissociation to CH was varied between 40 and 60% of k_1[e]. Hence four variables were used to adjust the model concentrations, namely, two sticking coefficients and two k[e] values.

The modeling calculations were carried out for a single mixture of 4:3:3 methane/hydrogen/oxygen. A primary objective of the modeling was to determine the most significant reactions contributing to the observed stable molecule concentrations. It was found that many of these changed by less than half an order of magnitude under different plasma conditions, and this precision was used as the criterion of modeling accuracy. Generally good agreement was obtained between measured and calculated concentrations as shown in Table 7. It was found that when O and H atom concentrations were in the range of 0.9 to 1.5 $\times$ 10^{13} cm^{-3} with sticking coefficients of 0.05 to 0.2 and 0.01 to 0.05, respectively, the calculated and measured concentrations agreed to better than 50%. These concentrations of atomic oxygen and hydrogen are entirely reasonable under plasma conditions and correspond to 0.4−1% dissociation of

the H_2 or O_2 added to the plasma. The hydrogen atom concentrations are of the same order of magnitude as calculated by Gogolides et al.[17](10^{13} cm^{-3}) in an rf methane plasma at 140 mTorr. The optimum values of the other variables required to produce the experimentally observed concentrations, the electron impact dissociation rate coefficients, k_{ie}, are given in Table 6. Last, when reactions involving CH_2 were included in the model they gave $[CH_2] \sim 10^9-10^{10}$ cm^{-3}, i.e., at least a 100-fold decrease on $[CH_3]$, as found by Gogolides et al.[17]

4. Discussion

4.1 Selection of Electron Impact and Neutral−Neutral Reactions. The neutral reactions chosen for modeling were selected from the known chemical composition of the plasma and also the selected plasma temperature. Certain neutral reactions having large activation energies were excluded. The role of molecules such as ethylene is therefore likely to be quite different from their reactivity in combustion or in high-temperature plasmas. A second criterion for selection was the measured or likely concentration of small species such as C, CH, and CH_2. Although their concentrations might be low, their reactions may nevertheless be rapid and they could make a significant contribution to the stable molecule concentration. For example, the CH radical reacts rapidly with CH_4 to form ethylene (Table 4, reaction 11) and may be a major contributor to ethylene formation. In contrast the reaction of CH with another low concentration species such as CH_2 can be ignored.

Although the ion−molecule rate constants are large these reactions were not included in the model, mainly because the ion concentrations were unknown. Furthermore their inclusion would significantly increase the number of variables in the model. The ion concentrations are estimated to be less than 10^{10} cm^{-3} and the 2*f* detection method is insufficiently sensitive to detect them. If the plasma contained a predominant cation, one way of circumventing this problem would be to equate the cation and electron densities. However, it is well-known that the initially formed CH_4^+ and CH_3^+ cations react rapidly, e.g., $CH_4^+ + CH_4 = CH_3 + CH_5^+$. Sugai et al.[26] found that a methane rf plasma at 123 mTorr contained CH_4^+ (4.1%), CH_3^+ (3.7%), CH_5^+ (33%), and $C_2H_5^+$ (39%). When oxygen is also present even more cations are formed, making it yet more difficult to include ion−molecule reactions in the model.

As mentioned earlier the variables in the model are the H and O atom concentrations and the electron impact terms. The electron impact parameters, k_{ie}, are given in Table 6, and the most important one is that for producing methyl from methane, k_{1e}, because all of the other electron impact reactions have been arbitrarily referenced to it. The value of k_{1e}[e] required in the model (0.45 s^{-1}) is considerably larger than that deduced from experiment for a pure methane plasma which was $\leq 0.1 s^{-1}$. This is probably due to the presence of oxygen in the plasma and would correlate with the proposed increase in the average electron energy due to a larger cathode fall potential. With an electron density of 10^{10} cm^{-3}, the average electron energy is ~3.1 eV which is a reasonable value for the negative glow.

4.2 C-2 Hydrocarbons. The dominant reaction forming ethane is recombination of methyl radicals (Table 4, reaction 2) so that an increase in the ethane concentration when oxygen was added (Figure 6) is to be expected because the methyl concentration also rises. The form of the decay profiles of the two species as more O_2 was added suggests that the removal processes are different in each case. Methyl reacts rapidly with oxygen atoms to produce formaldehyde (Table 4, reaction 20) while ethane reacts relatively slowly, particularly with the oxygen atom (reaction 29), and its concentration is controlled by electron impact and transport processes. The effect of transport can be examined qualitatively by changing the diffusion coefficients in the model. For methyl the concentration is virtually unchanged while the ethane concentrations are very sensitive to changes in the ethane diffusion coefficient. Further modeling shows that for ethane, electron impact dissociation and transport are almost equally important loss processes.

The abstraction of hydrogen atoms from ethane to produce the ethyl radical and then ethylene is too slow to be important at room temperature. An alternative source of C_2H_4 is the rapid reaction of the CH radical with methane (Table 4, reaction 11) which has a high rate coefficient at 325 K (~10^{-10} cm^3 $molecule^{-1}$ s^{-1}). Although the CH concentrations might be low, even if $[CH] = 5 \times 10^8$ cm^{-3} it would be high enough to produce the measured amounts of ethylene. Unfortunately the low concentrations of CH make its in situ detection by TDLAS very difficult. Like ethane, ethylene is removed by transport and electron impact dissociation to yield the vinyl radical and acetylene (Table 6, reactions 5 and 6). The slow decline in $[C_2H_4]$ when oxygen was added may be due to the destruction of CH by O or O_2.

The measured concentration of acetylene in the plasma is only slightly lower than that of ethylene. According to the model the largest source of acetylene is electron impact dissociation of ethylene, with the reaction $H + C_2H_3$ a minor route. The vinyl radical concentration is low and cannot be accurately modeled because its reactions have not been extensively studied, i.e., there are probably insufficient numbers of them for reliable modeling. Supplementary experiments were carried out to determine whether the acetylene concentration was linked to the presence of ethane. To test this idea the well-known free radical scavenger NO_2 was added to the plasma. The acetylene concentration was virtually unaffected by adding NO_2 in contrast to its effect on the methyl radical which declined sharply. This strongly supports the hypothesis that the acetylene does not arise from ethane. In contrast acetylene is formed in hydrocarbon combustion by H atom addition and abstraction reactions which proceed rapidly at elevated temperatures. The variation of acetylene concentration with added oxygen (Figure 6) mirrors that of ethylene presumably because of similar formation and removal reactions.

4.3 Formaldehyde, Methanol, and Formic Acid. TDLAS has enabled these three molecules to be detected for the first time in $CH_4-H_2-O_2$ ac and microwave plasmas, and their concentrations measured. Formaldehyde is one of the primary products of the plasma, formed in the early stages of the reaction sequence by the rapid step $O + CH_3 = CH_2O + H$ ($k_{20} = 1.4 \times 10^{-10}$ cm^3 $molecule^{-1}$ s^{-1}). It is removed by reaction with H, O, and OH to form the HCO free radical, and also by electron impact. Under oxygen-rich conditions where atomic oxygen plays the dominant reactive role the concentration of formaldehyde is given approximately by $[CH_2O] = k_{20}[CH_3]/k_{22}$ if we put $[CH_3]$ in the stationary state. Assuming $[CH_3] \sim 2 \times 10^{12}$ cm^{-3} then $[CH_2O] = 1.2 \times 10^{15}$ cm^{-3}. This number is about four times greater than the fully modeled value, indicating the importance of including even minor steps in the modeling calculations. Under conditions where the atomic oxygen controls the stationary concentration of formaldehyde then $[CH_2O]$ is independent of the oxygen flow (Figure 7) but depends on $[CH_3]$. This could explain the increase in $[CH_2O]$ when the methane content of the plasma was increased.

The reaction forming methanol is believed to be the third body process $CH_3 + OH + M = CH_3OH + M$, which under

plasma conditions has a rate constant of $\sim 1 \times 10^{-11}$ cm^3 molecule^{-1} s^{-1} at 1 Torr pressure. If this is the source of methanol then the reaction $O + CH_4 = CH_3 + OH$ is the initial but indirect source, so that higher concentrations of methyl radicals and oxygen atoms favor the formation of methanol. The rise in methanol concentration with added oxygen at the higher methane pressure (Figure 7) can be attributed to higher concentrations of OH. The most favorable conditions for forming OH in the plasma is when $[H_2] \sim [O_2]$. The addition of oxygen drives the ratio $[O_2]/([H_2] + [CH_4])$ closer to unity hence increasing [OH] (assuming that methane is also an indirect source of H_2). In contrast to formaldehyde the removal of methanol in the plasma is governed by transport and electron impact terms because its reactions with O, H, and OH are relatively slow (Table 4). Because all three reactions produce the methoxy free radical it would be interesting to try to detect this species in the plasma under high methanol conditions.

A second free radical which should also be present in small concentrations is HOCO. This intermediate is formed by three body combination of OH and CO and then decomposes to $H + CO_2$. If it is sufficiently long-lived it may react with H atoms, $HOCO + H + M = HCOOH + M$, to give formic acid. The rate constant of this reaction is unknown but can be estimated using transition state theory. If about 5% of the estimated concentration of HOCO reacts to give formic acid this gives a reasonable value for the concentration of the acid, $\sim 7 \times 10^{12}$ cm^{-3}. A second possible source of formic acid is the reaction of oxygen atoms with formaldehyde to give formic acid rather than HCO. The loss processes are again electron impact and transport. The formic acid signal decayed in much the same way as methanol when the oxygen or methane flow was extinguished, suggesting that it was formed in the gas phase rather than heterogeneously.

4.4 CO and CO_2. At low pressures of methane both CO and CO_2 concentrations were independent of the oxygen flow rate while at higher methane pressures an approximately linear dependence was observed (Figure 8). The main source of CO is the reaction $HCO + O_2 = CO + HO_2$, with reactions of HCO with O, H, and OH making lesser contributions. The concentration of CO_2 was always less than that of CO under all conditions, and the close similarity between [CO] and $[CO_2]$ with increasing pressure of oxygen suggests that the main reaction forming CO_2 is $OH + CO = CO_2 + H$. The concentrations of CO_2 formed were of the order of 10% of the methane consumed (measured in separate experiments). The agreement between experimental and modeled concentrations is satisfactory for both CO and CO_2 (Table 7). In the microwave plasma the relative concentrations of CO and CO_2 are about the same order of magnitude as here with respect to other product molecules. However, $[CO] > [CO_2]$ only at low oxygen flow rates with the opposite occurring at higher oxygen content. Also $[CO_2]$ is larger with respect to the amount of methane consumed. Both of these observations can be accounted for by the higher power dissipation in the microwave plasma.

4.5 Predicted Concentrations of OH and HCO. Apart from the methyl radical the concentrations of other transient species can be predicted from the modeling, and among the most important are OH and HCO which should have concentrations of order 5×10^{11} and 2×10^{11} cm^{-3}, respectively. The predicted concentration of OH is only four times lower than that of methyl itself so that it should be detectable. Unfortunately the origin of the OH fundamental band is ~ 3500 cm^{-1} which is a difficult region for TDLAS. The concentration of HCO is probably too low to detect by 2*f* modulation. This experimental limitation is unfortunate given that HCO is such an important intermediate for reactions leading to CO and CO_2.

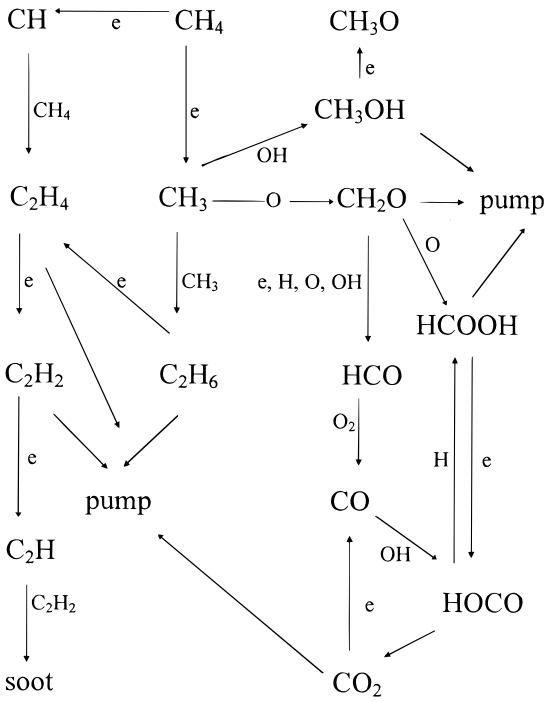

Figure 12. Important reactions for forming the species detected in a $CH_4-H_2-O_2$ ac plasma.

5. Concluding Remarks

The numerous reactions given in Table 4 can be reduced to a subset containing the most relevant neutral reactions accounting for the molecules detected in the plasma so far. Table 5 gives these reactions and Figure 12 is a diagrammatic representation of this set which is analogous to that of the model used by Kline et al.[15] but including the oxidative steps. To provide further information using the model more data are required on the electron densities and energy distributions. Experimental concentrations of other transient species, particularly H, O, OH, and HCO are required to develop the chemical input to the modeling. It must be emphasized that the model developed here represents only a qualitative description of the very complex plasma chemistry. It is nevertheless a useful guide for selecting plasma conditions and gas flows to maximize various species concentrations for film growth. It also provides a semiquantitative picture of the processes occurring in complex chemical systems such as ac and microwave $CH_4-H_2-O_2$ plasmas.

Acknowledgment. We thank the Oppenheimer Fund and Peterhouse, University of Cambridge, for the support of W.Y.F. This project formed part of the DAAD, British Council Joint Research Project 572 for which we are grateful. We thank Dr. E. Gogolides for helpful correspondence.

References and Notes

(1) Angus, J. C.; Koidl, P.; Dorritz, S. *Plasma Deposited Thin Films*; Mort, J., Jansen, F., Eds.; CRC Press: Boca Raton, 1986.

(2) Konuma, M. *Film Deposition by Plasma Techniques*; Springer-Verlag: Berlin, 1992.

(3) Fan, W. Y.; Röpcke, J.; Davies, P. B. *J. Vac. Sci. Technol. A.* **1996**, *14*, 2970.

(4) Yalamanchi, R. S.; Harshavardhan, K. S. *J. Appl. Phys.* **1990**, *68*, 5941.
(5) Hirose, Y.; Amanuma, S.; Komaki, K. *J. Appl. Phys.* **1990**, *68*, 6401.
(6) Yamada, C.; Hirota, E.; Kawaguchi, K. *J. Chem. Phys.* **1981**, *75*, 5256.
(7) Davies, P. B.; Martineau, P. M. *Appl. Phys. Lett.* **1990**, *57*, 237.
(8) Okeke, L.; Stori, H. *Plasma Chem. Plasma Proc.* **1991**, *11*, 489.
(9) Röpcke, J.; Mechold, L.; Käning, M.; Fan, W. Y.; Davies, P. B. *Plasma Chem. Plasma Process.* **1999**, *19*, 395.
(10) Davies, P. B.; Martineau, P. M. *J. Appl. Phys.* **1992**, *71*, 6125.
(11) Herzberg, G. *Molecular Spectra and Molecular Structure, Vol. II: Infrared and Raman Spectra of Polyatomic Molecules*; Van Nostrand Reinhold Co.: New York, 1945.
(12) Haverlag, M.; Stoeffels, E.; Stoeffels, W. W.; Kroesen, G. M. W.; De Hoog, F. J. *J. Vac. Sci. Technol. A.* **1996**, *14*, 380.
(13) Holbrook, K. A.; Pilling, M. J.; Robertson, S. H. *Unimolecular Reactions*, 2nd ed.; Wiley and Sons: New York, 1996.
(14) Yamada, C.; Hirota, E. *J. Chem. Phys.* **1983**, *78*, 669.
(15) Kline, L. E.; Partlow, W. D.; Bies, W. E. *J. Appl. Phys.* **1989**, *65*, 70.
(16) Semaniak, J.; Larson, A.; Le Padellec, A.; Stromholm, C.; Larsson, M.; Rosen, S.; Peverall, R.; Danared, H.; Djuric, N.; Dunn, G. H.; Datz, S. *Astrophys. J.* **1998**, *498*, 886.
(17) Gogolides, E.; Mary, D.; Rhallabi, A.; Turban, G. *Jpn. J. Appl. Phys.* **1995**, *34*, 261.
(18) Sugai, H.; Toyoda, H. *J. Vac Sci. Technol A.* **1992**, *10*, 1193.
(19) FACSIMILE manual; AEA Technology Harwell, 3rd ed., 1995.
(20) Moller, W. *Appl. Phys. A* **1993**, *56*, 527.
(21) Grill, A. *Cold Plasmas in Materials Fabrication*: *from fundamentals to applications*; IEEE Press: Piscataway, NJ, 1994.
(22) Baulch, D. L.; Cobos, C. J.; Cox, R. A.; Esser, C.; Frank, P.; Jut, Th.; Kerr, J. A.; Pilling, M. J.; Troe, J.; Walker, R. W.; Warnatz, J. *J. Phys. Chem. Ref. Data*, **1992**, *21*, 411.
(23) Nakano, T.; Toyoda, H.; Sugai, H. *Jpn. J. Appl. Phys.* **1991**, *30*, 2908.
(24) Cali, F. A.; Herbert, P. A. F.; Kelly, W. M. *J. Vac. Sci. Technol. A* **1995**, *13*, 2920.
(25) Dagel, D. J.; Mallouris, C. M.; Doyle, J. R. *J. Appl. Phys.* **1996**, *79*, 11.
(26) Sugai, H.; Kojima, H.; Ishida, A.; Toyoda, H. *Appl. Phys. Lett.* **1990**, *56*, 2616.